

PAPER • OPEN ACCESS

## Assessing potential coastal flood exposure along the Port-Bouët Bay in Côte d'Ivoire using the enhanced bathtub model

To cite this article: Marcel Kouakou *et al* 2023 *Environ. Res. Commun.* **5** 105001

View the [article online](#) for updates and enhancements.

You may also like

- [Dependence of instability to induce a bathtub vortex in a rectangular vessel on the aspect ratio of the horizontal cross section](#)  
Jiro Mizushima, Rei Matsuda and Naoto Yokoyama
- [Sea level rise and coastal flooding threaten affordable housing](#)  
Maya K Buchanan, Scott Kulp, Lara Cushing et al.
- [A review of estimating population exposure to sea-level rise and the relevance for migration](#)  
Celia McMichael, Shouro Dasgupta, Sonja Ayeb-Karlsson et al.

## Environmental Research Communications



## PAPER

## Assessing potential coastal flood exposure along the Port-Bouët Bay in Côte d'Ivoire using the enhanced bathtub model

## OPEN ACCESS

## RECEIVED

9 July 2023

## REVISED

24 September 2023

## ACCEPTED FOR PUBLICATION

27 September 2023

## PUBLISHED

11 October 2023

Original content from this work may be used under the terms of the [Creative Commons Attribution 4.0 licence](#).

Any further distribution of this work must maintain attribution to the author(s) and the title of the work, journal citation and DOI.

Marcel Kouakou<sup>1,\*</sup>, Jacques André Tiémélé<sup>2</sup>, Éric Djourou<sup>2</sup> and Kissao Gnandi<sup>3</sup>

<sup>1</sup> West African Science Service Centre on Climate Change and Adapted Land Use (WASCAL) Graduate Research Program on Climate Change and Disaster Risk Management, Department of Geography, University of Lomé, Lomé, Togo

<sup>2</sup> Centre Universitaire de Recherche et d'Application en Télédétection (CURAT), Université Felix Houphouët Boigny, Abidjan, Côte d'Ivoire

<sup>3</sup> Department of Geology, University of Lomé, Lomé, Togo

\* Author to whom any correspondence should be addressed.

E-mail: [kouakou.m@edu.wascal.org](mailto:kouakou.m@edu.wascal.org)**Keywords:** coastal flood, Port-Bouët Bay, enhanced bathtub model, flooding exposure, climate change**Abstract**

Coastal flooding is a growing concern for many communities worldwide due to climate change. This study focuses on the Port-Bouët Bay, located in Abidjan, Côte d'Ivoire. A coastal flood model based on the enhanced bathtub model was used to map the present and future flood extent and assess exposure to quantify the likely affected populations, buildings, and land uses for different scenarios. The model incorporated a digital elevation model, surface roughness, flood water source, and the once a century extreme sea-level scenarios. Validation was conducted against GPS coordinates of recently flooded zones. The analysis revealed that, under current conditions, around 21.58 hectares are vulnerable to flooding, and approximately 2465 people and 544 buildings are exposed to flooding today. Based on future projections, the extent of flooding is anticipated to increase by different ranges depending on the time period and the climate change conditions. By the end of the century, the increase in flooding extent could reach a percentage of 27%, 37%, and 90% under SSP1-2.6, SSP2-4.5, and SSP5-8.5, respectively. The impacts would consequently be worsened with greater number of people and assets exposed to future coastal flood hazard. The land use analysis showed that informal settlements are the occupation most exposed, followed by residential settlements, commercial and industrial land, in that order. The spatial disaggregation of this exposure across neighborhoods indicates that Sogefiha is the most exposed, followed by Petit-Bassam and Vridi. However, a substantial increase in coastal flooding in Vridi by 2100 under the SSP5-8.5 scenario could lead to significant exposure level change for this scenario. This information is critical for evaluating and managing present and future coastal flood risks in the Port-Bouët Bay area and for informing decision-making processes.

**1. Introduction**

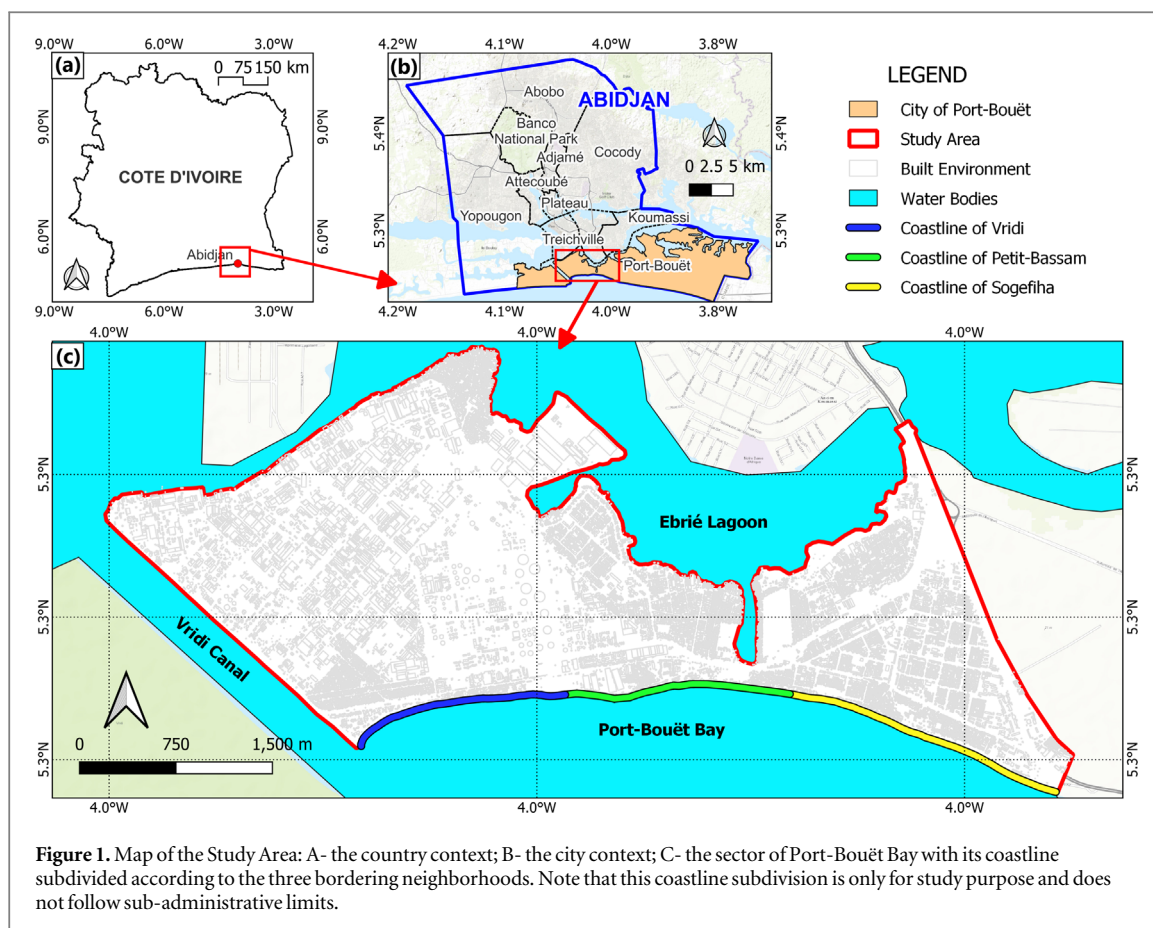
Coastal zones are dynamic and valuable ecosystems that provide numerous opportunities for human development (Castillo *et al* 2012, Lakshmi, 2012). They offer important economic benefits such as fisheries, shipping, tourism, and have significant cultural and recreational values. These are the reasons why approximately 40% of the global population reside within these areas (United Nations 2017). However, coastal zones are vulnerable to a range of natural hazards (Al Ruheili and Boluwade 2023) among which coastal flood have historically been one of the deadliest and most damaging worldwide (Idier *et al* 2020). In a broader sense, coastal floods refer to the flooding that occurs in coastal zones (Fang and Shi 2021). But, for the purpose of this study, it is defined as natural phenomenon where coastal areas become permanently or temporarily submerged by the nearby sea (D'Arcy *et al* 2022). It suddenly occurs when the meteorological conditions are sufficiently severe and the sea levels extremely high to overtop or breach coastal defences (dunes, dikes) and cause inundation of low-lying areas. This type of flooding leaves little time for warning and preventative evacuation,

and often results in significant impacts, including damage to coastal infrastructure and ecosystems, harm to human health, and disruption of people's lives (World Meteorological Organization, 2013, Steffen *et al* 2014).

Over the past few decades, coastal flood events have become increasingly frequent and intense in many parts of the world (e.g., Dube *et al* 2022, Hague *et al* 2022). The scientific community widely agrees that these trends are primarily due to human activity, both direct impacts such as urbanization and navigational development, and indirect impacts such as rising sea levels and hydroclimate extremes resulting from climate change (Kirwan and Megonigal, 2013 Vitousek *et al* 2017, Wahl *et al* 2017, Wu *et al* 2017, Alizad *et al* 2018, Vousdoukas *et al* 2018). As climate and anthropogenic changes are projected to increase the vulnerability of coastal areas (Neumann *et al* 2015, IPCC, 2021), the impacts of coastal flood hazard could become increasingly worse in the future (Hallegatte *et al* 2013, Vitousek *et al* 2017), with more places, people and assets threatened by the phenomenon. Without strategic adaptation measures, an estimated 0.2% to 4.6% of the global population may be exposed to coastal flooding (Kulp and Strauss 2019). These predictions underscore the urgency of addressing coastal flood risks and supporting stakeholders in implementing effective risk reduction strategies.

As a key component of coastal flood risk, exposure assessments help by providing vital information about populations and assets located within flood-prone areas. This information is essential for coastal communities and decision-makers as it forms the basis for developing plans and interventions related to preparedness, early warning, response, recovery, and mitigation (HARPIS-SL 2022). Analyzing exposure enables us to generate insights into the potential impacts of coastal flooding. Flood mapping is typically used in conjunction with exposure analysis to detect areas likely to be flooded and categorize them for more effective analysis. While generating flood maps of past events is relatively straightforward, creating present and future maps requires prediction based on models which, provide a comprehensive view of flooding characteristics at different spatial and temporal scales. Overall, exposure assessment and flood mapping are critical tools for understanding and managing coastal flood risk.

Many models have been developed and applied for coastal flood simulations in recent decades. Two common approaches in the approaches in the literature are the bathtub model (BTM) and the hydrodynamic model (HDM) (Neumann and Ahrendt 2013). Each of these models has its own strengths and limitations, and the choice of which approach to use largely depends on the intended purpose and data availability. HDMs simulate coastal flooding by solving mathematical equations such as the 2D/3D shallow water equations. This approach accounts for the dynamic aspect of physical processes leading to flooding, and therefore requires detailed input conditions, specialized software (e.g., DELFT-3D, MIKE-3D) and skills. HDMs can be complex and result in longer computational times (Amante 2018). They are commonly used for flood forecasting (Gallien *et al* 2014) and the planning and implementation of flood protection measures (Ward *et al* 2011). On the other hand, BTMs adopt a hydrostatic approach. They offer computational efficiency and are valuable for quickly identifying flood-prone regions based on specific flood water levels. BTMs are frequently employed in conjunction with geographic information systems (GIS) and can be executed using raster calculations (Seenath *et al* 2016). There are two main types of BTMs: the standard BTM (sBTM) and the enhanced BTM (eBTM). sBTM assumes that flood occurs in all areas with land surface elevation below the flood water level, regardless of hydrological connectivity to the coast (Poulter and Halpin 2008, Fereshtehpour & Karamouz 2018). In contrast, the eBTM accounts for hydrological connectivity with the flooding source and integrates terrain aspects and slopes (Williams and Lück-Vogel 2020). As an improved version of the sBTM, the eBTM not only offers a simplified approach but also provides a more precise representation of flooding scenarios. The Port-Bouët Bay in Côte d'Ivoire is among the areas increasingly threatened by coastal flood impacts. It faces particularly high exposure due to a combination of factors, including coastal population growth, expanding economic activities, limited and inadequate coastal protection infrastructure, and the intensifying frequency and severity of extreme sea level events driven by climate change (IMDC 2017, Nicholls *et al* 2007, World Bank 2020). The area has experienced multiple coastal flood events, including the documented 2011 flood that destroyed hundreds of homes and left more than a thousand families without shelter (Sadia 2014). However, limited information on current and future coastal flood exposure hinders the development and planning of effective strategies for local risk reduction and adaptation. This study thus intends to contribute to improving the understanding of the changing risk trend of this hazard within the Port-Bouët Bay and support decision-making. The objective is twofold. Firstly, we seek to identify present and future flood-prone areas using the eBTM as simulation tool model and secondly, we aim to comprehensively assess the populations, buildings and land-uses covered by the flood. While making distinction between population and assets (buildings and occupations) in the context of this study, it is crucial to recognise their inherent connection within the context of exposure assessment.



## 2. Study area

The Port-Bouët Bay area, situated in the Southeast of Côte d'Ivoire, is a peninsula that forms the central section of Port-Bouët, one of the ten towns comprising the Ivorian capital Abidjan. The bay is bounded by the lagoon Ebrié to the north and the Atlantic Ocean to the south, and spans 5.5 km from the Vridi canal to the city's lighthouse, as shown in figure 1. Its geographical coordinates lie between latitudes 5.248 °N–5.280 °N and longitudes 4.022 °W–4.952 °W. The Port-Bouët Bay, which covers an area of 11.5 km<sup>2</sup>, is home to around 97,000 people, accounting for approximately 16% of Port-Bouët's population. The population of this area, much like that of the entire city, is increasing rapidly at a rate of 5.7% per year (INS, 2014; 2021). The terrain is relatively flat, with almost all of the bay being below 8 m in elevation (JICA, 2015), making it a Low Coastal Zone (LCZ) that is susceptible to frequent and severe coastal flooding. Over the past few decades, the area has undergone significant socioeconomic changes, with the development of various industries and homes leading to the hyper-urbanization of the coast. Port-Bouët Bay's urban landscape is characterized by a mix of essential infrastructure such as port facilities and industries, as well as pockets of informal settlements. Based on the bordering neighborhoods, the coastline can be divided into three: Vridi, Petit-Bassam, and Sogefiha, from west to east as shown in figure 1. Note that these neighborhoods will serve as the local units for our assessment.

## 3. Data and methods

This study follows a two-step methodology that encompasses coastal flood modeling and exposure analysis. The first step involves generating flood maps using the enhanced Bathtub Model (eBTM), which integrates extreme sea level (ESL) conditions with the local morphological features. The second step involves overlaying the flood maps generated in the first step with the land use and population maps of the study site. This enables the estimation of coastal flood exposure, which is the number of people and assets at risk due to flooding. Figure 2 provides a schematic representation of the methodology shortly described above. In the following paragraphs, a more detailed description of each of the two steps is provided.

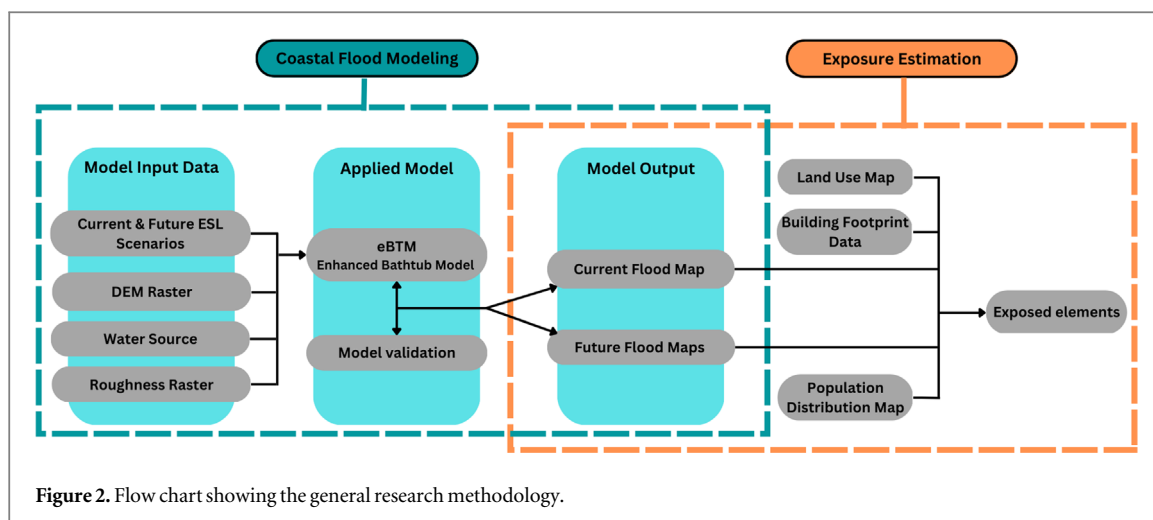


Figure 2. Flow chart showing the general research methodology.

### 3.1. Coastal flood modeling

#### 3.1.1. Modelling approach

In this work, the eBTM serves as the framework for conducting various coastal flood simulations. The model, conceptualized by Williams (2019) and developed in ESRI ArcGIS software, aims to address temporary coastal inundation and the lack of easily accessible, user-friendly tools (Williams and Lück-Vogel, 2020). It is important to note that the eBTM, being a GIS-based model, focuses on capturing the dynamics within its scope, and while it may not encompass all aspects of physics like more advanced hydrodynamic models, it offers a valuable approach for understanding and assessing coastal flood scenarios. The model as tested and validated in Strand, a municipality in Cape Town, South Africa, is the eBTM module with homogeneous roughness (Williams and Lück-Vogel 2020). However, a module with roughness raster (non-homogeneous) is also provided in the toolbox. This latter module, which reflects a growing body of GIS tools applicable to the coast, will be used in the context of this study. To conduct flooding simulations using the eBTM, four input datasets are essential: the digital elevation model (DEM), water source, surface roughness, and flood water level. The next section provides a detailed description of each of these crucial datasets.

#### 3.1.2. Model inputs data

##### 3.1.2.1. Digital elevation model (DEM)

For reliable coastal flood modeling, a high-resolution DEM is crucial (Gesch 2018). In our analysis, the Digital Elevation Model (DEM), specifically the digital terrain model (DTM), was obtained from topographic survey data collected in 2013 as part of the 'Digital Topographic Mapping Project for Urban Infrastructure Development' (JICA, 2015). The DTM represents the bare earth elevation, excluding any above-ground features (buildings and vegetations). The data was initially collected in point file format and covered 931 measurement points over the study site, with one point for every 11–12 m<sup>2</sup>. To obtain a continuous regular terrain elevation, this relatively coarse dataset was later interpolated to fill certain gaps. The resulting DEM has a resolution of 10 × 10 m and uses as vertical datum, the Abidjan mean sea level, which serves as the reference point for the port of Abidjan. While the resolution might seem coarse for coastal inundation modeling, it is important to recognize the data scarcity in the study area, compelling us to optimize the available DEM resources. Figure 3 provides a visual representation of the obtained Digital Terrain Model (DTM).

##### 3.1.2.2. Surface roughness

As eBTM is a GIS-based model, it should be noted that it does not directly address the detailed physics as a hydrodynamic or numerical model would. This means that certain factors, like wind-push effects, remain unaccounted for in this approach, unlike more sophisticated models. However, the model incorporates the roughness parameter of the terrain to address terrain slope's influence on water movement across the landscape. The eBTM offers two options for roughness input: a single-value roughness for the entire study site, used in the homogeneous roughness module, and space-varying values, used in the roughness module. However, in both cases, roughness values fluctuate between a minimum of 0 for smooth surfaces and a maximum of 1 for rough surfaces (Williams 2020). For this analysis, the roughness raster was used. The roughness raster file of the study area (see figure 4) was generated with the same resolution as the input DTM. As illustrated in figure 4, rough areas are prominently located along the coastline.

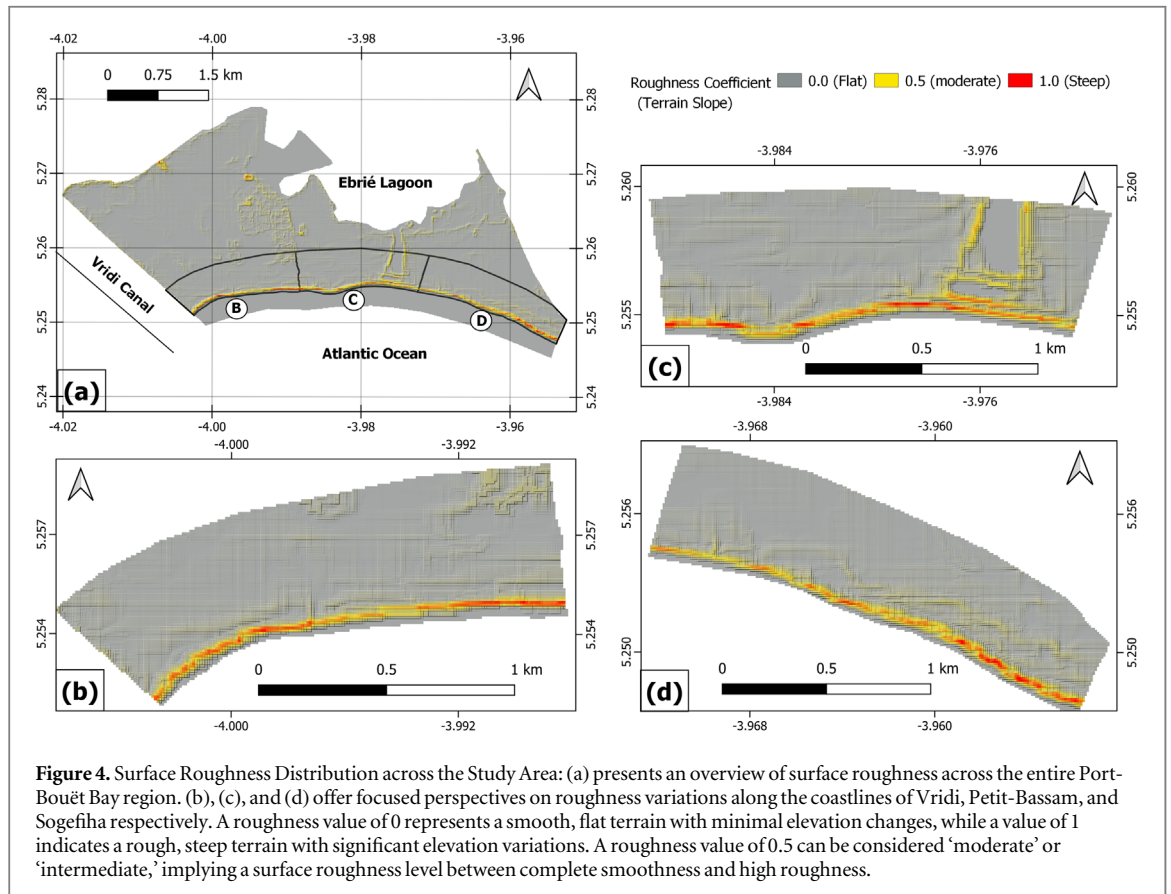
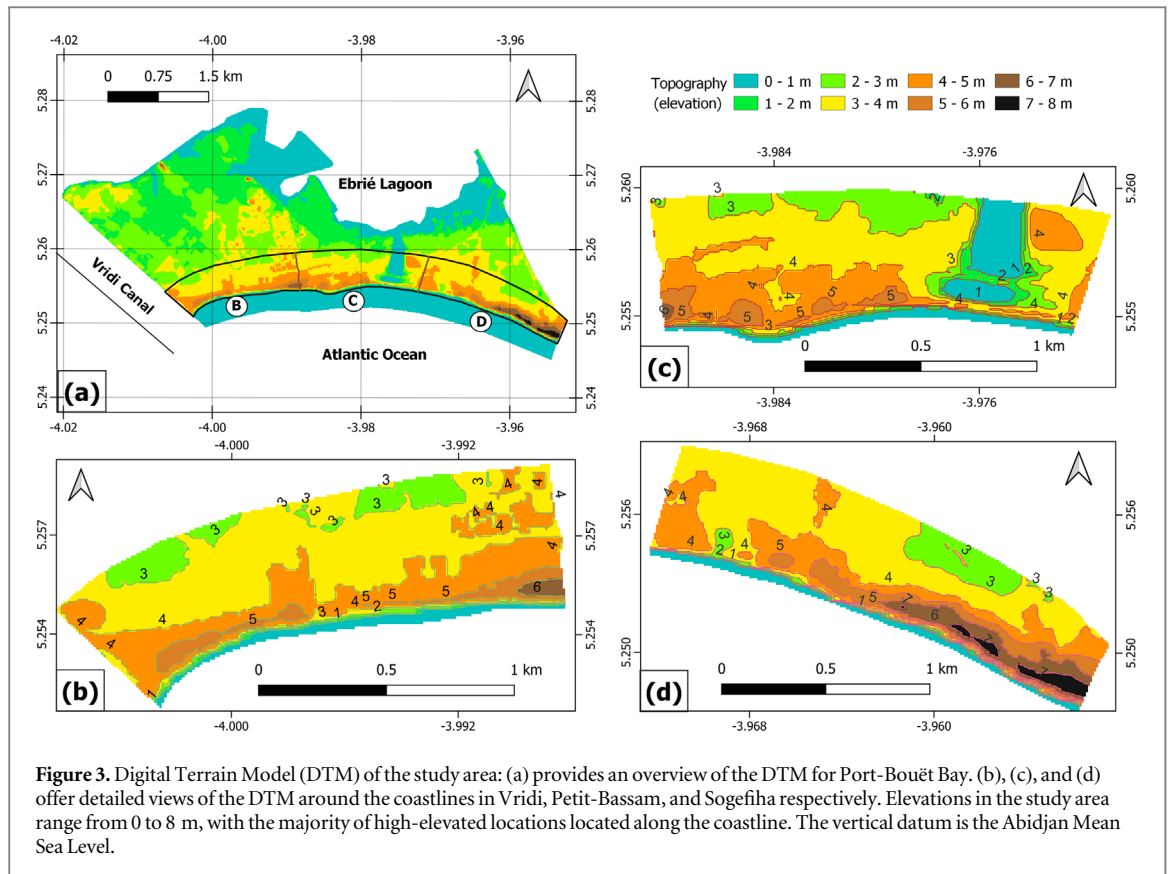


**Table 1.** Present and future 100-year return period of extreme sea level (ESL) at the scenarios used to run the eBTM model.

Location	Scenarios	Years			
		2020	2030	2050	2100
Vridi	SSP1-2.6	4.37 m	4.481 m	4.590 m	4.858 m
	SSP2-4.5		4.480 m	4.606 m	4.988 m
	SSP5-8.5		4.485 m	4.634 m	5.210 m
Petit-Bassam	SSP1-2.6	4.97 m	5.081 m	5.190 m	5.458 m
	SSP2-4.5		5.080 m	5.206 m	5.588 m
	SSP5-8.5		5.085 m	5.588 m	5.810 m
Sogefiha	SSP1-2.6	4.48 m	4.591 m	4.700 m	4.968 m
	SSP2-4.5		4.590 m	4.716 m	5.098 m
	SSP5-8.5		4.595 m	4.744 m	5.320 m

### 3.1.2.3. Water source

In eBTM modeling, the water source represents the initial position of the floodwater, establishing hydrological connectivity to the coast and providing a starting point for the water's inward propagation (Williams and Lück-Vogel 2020). To obtain the water source for this analysis, the zero-altitude shoreline along the coast was digitized from the input DEM (saved as a shapefile), ensuring that the water source intercepts the DEM to maintain hydrological connectivity to the coast (Williams 2020).

### 3.1.2.4. Flood water level scenarios

To determine the extent of land inundation during a coastal flood, it is necessary to input the floodwater level into the model. This study considered several scenarios, which were estimated from extreme sea level (ESL) conditions resulting from a combination of factors, including tide, storm surge, wave runup, and projected relative sea level rise (SLR). ESL values for three climate change scenarios, based on Shared Socioeconomic Pathways (see table 1) at the neighborhood scale, were obtained from Kouakou *et al* (2023). The present-day ESLs were determined by computing the statistical 100-year joint return values of storm tide (tide + storm surge) and wave runup. Future ESLs were predicted by integrating present-day ESLs with recent SLR projections based on SSPs, as detailed in Fox-Kemper *et al* (2021), Garner *et al* (2021a), and Garner *et al* (2021b).

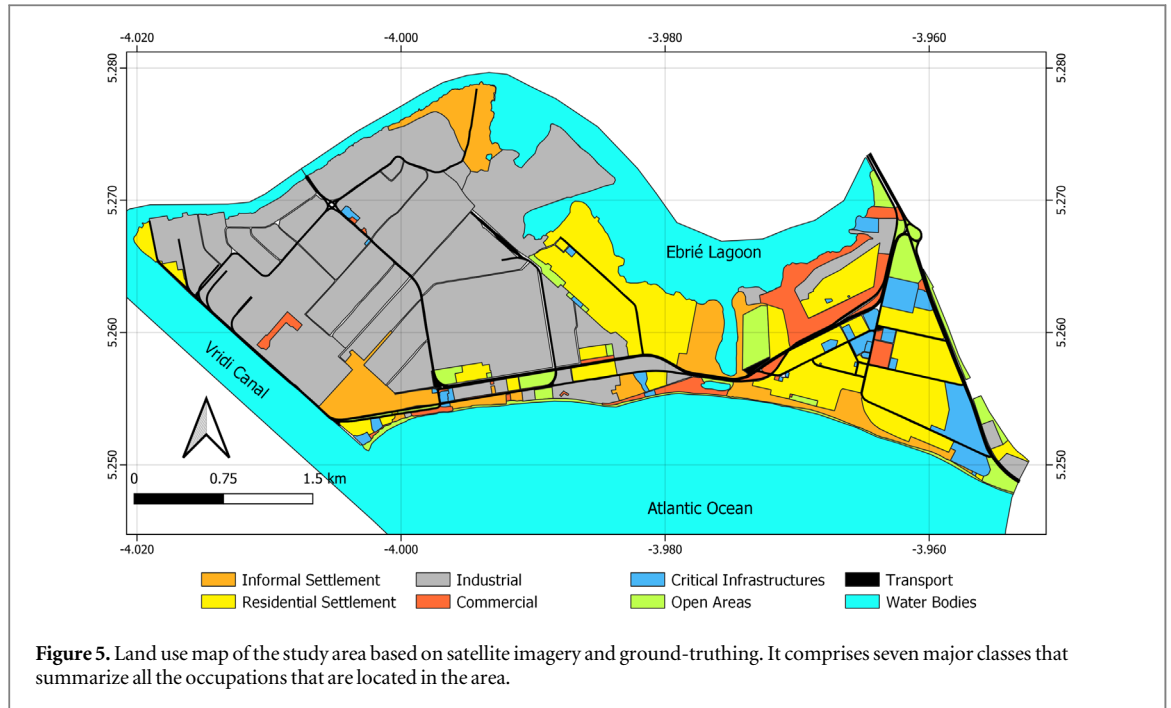
### 3.1.3. Model setup and validation

The model was configured with the assumption that input datasets such as topography, surface roughness, and water source will remain constant in the future, with only the flood water level changing over time. Since the input datasets are available for each coastline segment of the Port-Bouët Bay, the model simulations were executed individually for each neighborhood to produce the outputs for the corresponding periods. This approach of running separate models for each neighborhood helps ensure accurate representation and assessment of flood impacts for each distinct location. The output from each simulation was provided as a flood raster layer that is connected to the coast, indicating the water depths relative to the input DTM for each pixel. The flood layers were carefully reviewed to ensure that the working resolution is capable of producing results that align with the local flood patterns.

After the model was set up and the initial check, the next step was to evaluate the accuracy of the results. To achieve this, the model results were compared with GPS coordinates of areas that were recently flooded. During a ground survey, local residents were asked to indicate coastal flood limits for recent years or show the locations where they had personally experienced flooding. The GPS coordinates of these locations were collected and compared with the present-day modeled flood layer to determine any overlap. A total of twenty GPS points was collected for events that occurred between 2014 and 2020.

## 3.2. Exposure estimation

To assess the potential impact of floods on the urbanized area of the Port-Bouët Bay, it is necessary to determine the exposed elements (assets, populations and land-uses). This requires detailed data on these elements in a Geoinformatics format, along with coastal flood layers (Percival and Teeuw 2019). In this study, the used datasets were partially completed and needed some additional arrangements. The population data was downloaded from the 'Data for Good' platform (FCL and CIESIN 2022). This database provides global raster files of population estimates within 30-meter grid cells for the year 2020 using AI, satellite imagery, and census data. The development of these high-resolution maps relies on high-resolution identification of populated areas and a thorough understanding of the underlying population distribution patterns. To streamline the analysis,



the initially collected population raster file for the entire country was clipped to match the study area's extent and subsequently disaggregated to align with the resolution of the flood raster files ( $10 \times 10$  m). For simplicity purposes, the disaggregation process used the uniform disaggregation method, equally distributing population counts from the coarse grid to the finer grid cells. Since the acquired data represents the 2020 population count, which pertains to the present-day, future population data was derived through projections using equation (1).

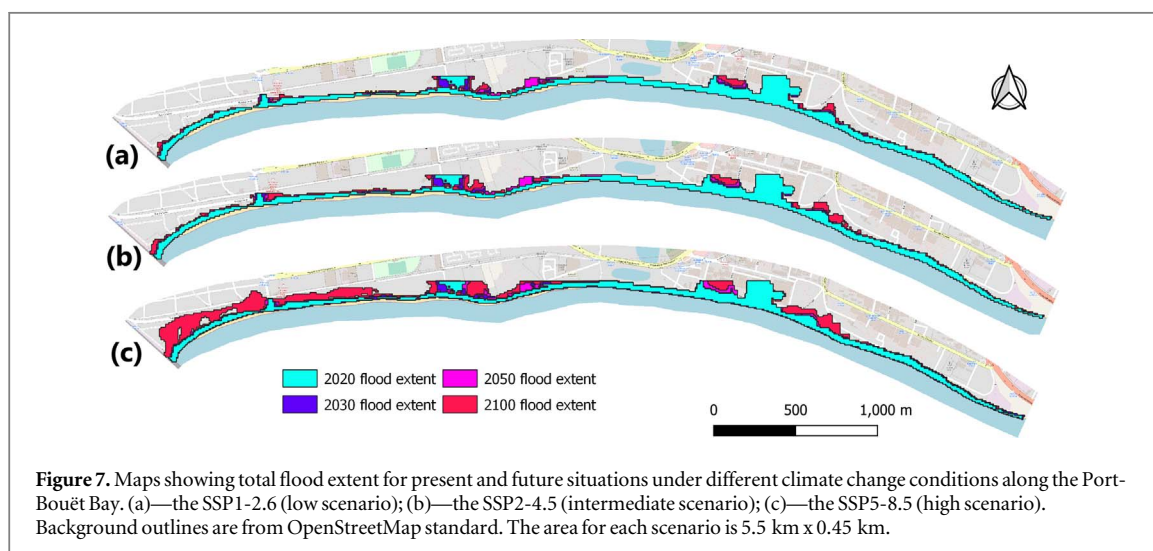
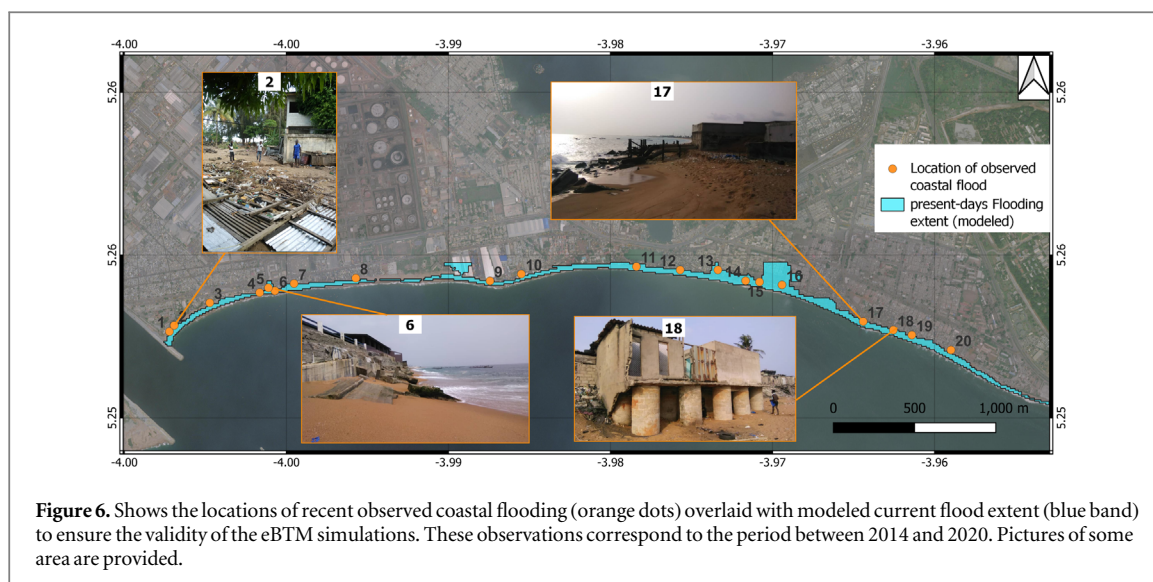
$$P_f = P_p \times (1 + R_m)^t \quad (1)$$

Where  $P_f$  is the future population;  $P_p$  is the present population;  $R_m$  is the average annual growth rate, and  $t$  is the projected number of years. The value of  $R_m$  was calculated using historical population data from CIESIN (2018), which provides past population estimates every five years from 2000 to 2020, along with equation (2) where  $P_i$  and  $P_{i-1}$  are respectively the ending and starting population count over the five-year period.

$$R_m = \sum \frac{\frac{P_i - P_{i-1}}{5 \times P_{i-1}}}{n} \quad (2)$$

In order to evaluate the potential number of buildings at risk of flooding, building footprints were incorporated into the exposure analysis using the 'open building' database (Sirko *et al* 2021). This database offers one of the most extensive building maps for the region. Additionally, each footprint in this database is assigned a confidence level, enabling manual adjustments for low-confidence footprints to achieve the most accurate real-world representation. In evaluating potential flood impacts on various occupations within the area, the land-use map was created by digitizing the different occupations within the study site. This process involved satellite imagery from OpenStreetMap and conducting guided field surveys to validate the accuracy of the data. The resulting occupations were then categorized into seven specific land use classes (refer to figure 5), including open area class that corresponds to unoccupied spaces. Notably, in figure 5, land-use types are assigned based on predominant occupations, and the color coding of the map adheres to the recommendations of Jeer and Bain (1997).

The exposure analysis for each scenario involved overlaying the respective flood layer with the population, building, and land use distribution maps of the study area. This allowed us to determine the number of people and buildings at risk, identify the likely affected land-use categories and estimate the flooded surface per land use. To conduct this analysis, we employed the zonal statistics approach, which involves aggregating data within flooded zones to gain insights into various attributes or characteristics. This technique provides a deeper understanding of how data is distributed and interacts within the flooded areas, contributing to a comprehensive evaluation of flood impacts for each neighborhood within our study area.



## 4. Results

### 4.1. Coastal flood mapping

Before presenting and commenting on the findings, the eBTM output for the present day was compared to the GPS coordinates of recently flooded areas, as described in the model validation section. The twenty collected observation points are plotted against the model output in figure 6. It emerged from this comparison that the model results match with about two-thirds of the observations. In the remaining one-third, the modeled coastal flood is underestimated. However, the spatial differences between the model and observations outside of the modeled flood extent were mostly less than 10 meters, i.e., an underestimation of just one pixel. Only two observations (point number 8 and 20) were found to be distant from the modeled flood limit by more than 10 meters (14 and 16 meters, respectively). After analyzing the simulation's resolution, it can be inferred that the observed distribution of coastal floods and the model results for the present day exhibit a general consistency. Consequently, the validity of the input datasets and the eBTM simulation in the Port-Bouët Bay can then be established.

Figure 7 and table 2 present a comprehensive overview of the simulation results across different climate change scenarios and years, illustrating the extent of the flooded areas within the Port-Bouët Bay. The visualizations in figure 7 offer clear evidence of the bay's vulnerability to flooding, primarily concentrated in areas adjacent to the shoreline. Currently, as of 2020, the simulations under the 100-year ESL return level reveal that the estimated flooded area is approximately 21.58 hectares (see table 2). The simulations project varying degrees of increased flooding in the coming decades. Over the next 10 years, a projected 5%–8% of additional

**Table 2.** Estimates of total flooded area (in hectares) per neighborhood and per scenario.

Location	Scenarios	Years			
		2020	2030	2050	2100
Vridi	SSP1-2.6	4.47 ha	4.63 ha	4.93 ha	5.64 ha
	SSP2-4.5		4.57 ha	5.03 ha	6.58 ha
	SSP5-8.5		4.84 ha	5.07 ha	18.62 ha
Petit-Bassam	SSP1-2.6	6.11 ha	6.82 ha	8.00 ha	8.84 ha
	SSP2-4.5		6.77 ha	8.00 ha	9.19 ha
	SSP5-8.5		7.14 ha	8.23 ha	10.76 ha
Sogefiha	SSP1-2.6	11.00 ha	11.43 ha	11.83 ha	13.06 ha
	SSP2-4.5		11.41 ha	11.89 ha	13.87 ha
	SSP5-8.5		11.47 ha	12.12 ha	15.24 ha

land would periodically be flooded during extreme sea level events. Looking ahead to 2050, the coastal flood extent is anticipated to rise by 14%–18% compared to the present state. Towards the end of the century, two specific scenarios, SSP1-2.6 and SSP2-4.5, may lead to flood increases of up to 27% and 37%, respectively. Particularly under SSP5-8.5, by the year 2100, figure 6(c) of the flood map strikingly displays a significant surge in coastal flooding, distinctly surpassing current conditions. The analysis underscores the potential doubling of the current flood extent by 2100 under SSP5-8.5. The detailed values for the different neighborhoods, scenarios, and years are exhaustively presented in table 2.

The information provided in table 2 provides evidence that the neighborhoods of Vridi, Petit-Bassam, and Sogefiha experience varying degrees of exposure to coastal flooding under different climate change scenarios and years. Among these neighborhoods, Vridi consistently exhibits the least exposure to coastal flooding across the scenarios and years. Notably, the SSP5-8.5 scenario for the year 2100 shows a significant increase in the flooded area, indicating the highest level of exposure under this particular climate change trajectory and year. In the case of Petit-Bassam, there is a moderate level of exposure to coastal flooding. While the projections for flooded areas increase across scenarios and years, the growth appears gradual, suggesting a steadier rise in flooding over time. Conversely, Sogefiha is consistently projected to experience the highest degree of exposure to coastal flooding among the three neighborhoods. The neighborhood's initial larger flooded area and its consistent expansion across all scenarios and years point to a heightened susceptibility to rising sea levels. Overall, this analysis suggests that Sogefiha is the most exposed neighborhood, followed by Petit-Bassam, and then Vridi.

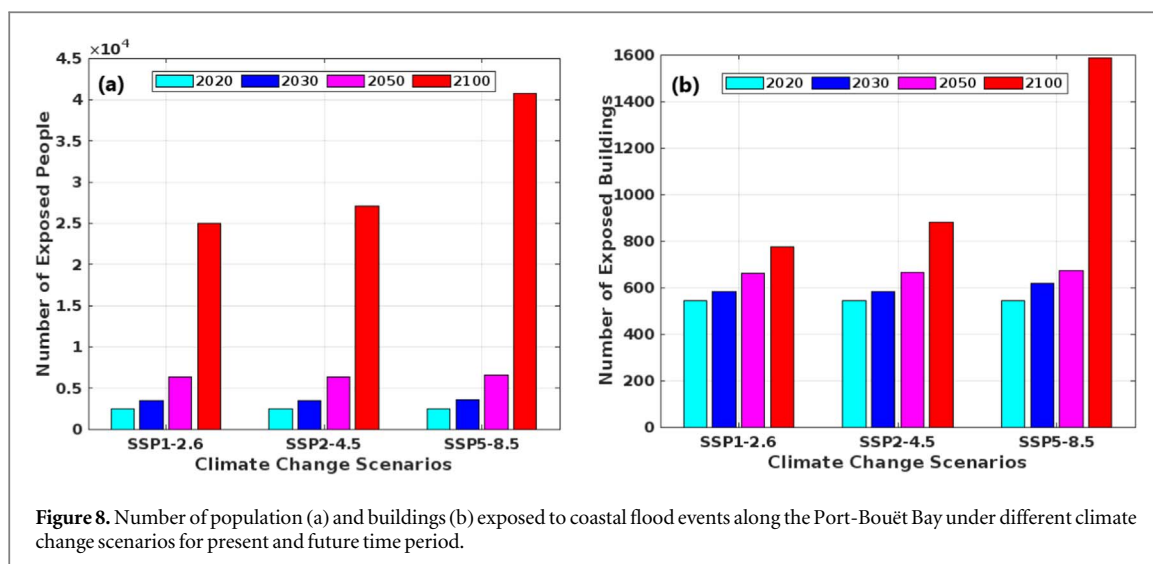
## 4.2. Coastal flood exposure

### 4.2.1. Exposed population and buildings

Based on the coastal flood extent discussed earlier, we have identified the population and buildings exposed to floodwaters. Figures 8(a) and (b) show the results for various climate change scenarios. From figure 8(a), around 2465 people are currently exposed to the once-a-century flood water level, with this number expected to increase due to demographic growth. By 2030, the increase will be between 42% and 45%, while by mid-century, it could reach 82% to 85%. Assuming that population growth remains the same, by 2100, the number of exposed individuals may be 24.93, 27.03, and 40.78 thousand under SSP1-2.6, SSP2-4.5, and SSP5-8.5, respectively.

Figure 8(b) indicates that roughly 544 buildings in the study area are exposed to coastal floods, with the majority being fully within the inundated zones. However, a subset of these buildings, situated at the outskirts of flood zones, would only experience partial exposure. Regardless of the scenario, the number of exposed buildings is expected to slightly increase from 2020 to 2050 under future climate change conditions. By end-century, under SSP1-2.6 and SSP2-4.5, the percentage of increase in flood-affected buildings would be 43% and 62% higher than the current scenario, respectively. However, under SSP5-8.5, the number of affected buildings could be almost three times more than the current scenario.

The analysis of exposed elements in each neighborhood, shown in figure 9, reveals distinct spatial patterns across scenarios. In Vridi, the current count of exposed population of 285 people gives way to divergent trajectories over time. By 2030, exposure increases by around 44%–51% compared to the baseline, with further escalation by 2050 (145%–163%). By the century's end, the exposed population reaches a significant magnitude, becoming nearly 46 times greater than the count in 2020 under scenario SSP5-8.5. In Petit-Bassam, the 817 people currently exposed rises by approximately 50%–53% by 2030, and projections for 2100 reaching 10 to 13 times higher. A parallel trend emerges in Sogefiha, where exposure climbs by about 36%–39% by 2030, rising to around 140%–146% by 2050 and may reach 8 to 11 times higher by the end of the century. Shifting focus to exposed buildings, noteworthy trends emerge. In Vridi, the initial building exposure count of 33 in 2020 experiences slight upticks by 2030 and 2050, followed by a significant surge by 2100. It is worth noting that the



number of buildings exposed to flooding could reach a staggering 670 by 2100 under the SSP5-8.5 scenario. Similarly, in Petit-Bassam, where exposure begins at 141 buildings, reaching 158 to 185 by 2030 and ascending to 221–278 by 2100. Likewise, in Sogefiha, building exposure starts at 370, remains steady at 392 by 2030, and increases to 43–426 by 2050, culminating at 498–637 by the close of the century.

#### 4.2.2. Exposed land-uses

In this subsection, we evaluated the distribution of land use in the flooded zones for each of the scenarios. Our findings reveal that, for the present-day 100-year return period of extreme sea level, the most exposed land use class is the open area (11.98 ha), followed by informal settlement (5.44 ha), residential settlement (1.82 ha), commercial (1.36 ha), industrial (0.74 ha), critical infrastructure (0.2 ha) and transport (0.02 ha), in that order. These distributions are primarily based on the dominant occupations within the flooded zones. Noteworthy, the significant proportion of exposed ‘open areas’ helps to mitigate the potential impacts of today’s coastal flood, as there are no significant assets in this land use class.

Under future climate change scenarios, as the flooded surface per land use increases, the ranking of occupations most or least exposed would remain similar to the current situation (see figure 10). This indicates that the exposure of all land use type would increase proportionally to the flooded surface. However, we note a negative trend (decrease) of the future flooded surface of ‘open areas’ over time, while the other land uses have a positive trend of flooded surface (increase). For instance, under SSP5-8.5 (refer to figure 10(f)), the relative share of ‘open areas’ decreases from 55.5% in 2020 to 35.2% in 2100, a decrease of about 20.3%, while there is an increase of 4.6% for ‘Industrial’ (from 3.5% to 8.1%), 4.5% for informal settlements (from 25.2% to 29.7%), 3.7% for ‘critical infrastructures’ (from 0.9% to 4.6%), 3% for ‘Commercial’ (from 6.3% to 9.3%), 2.7% for ‘Residential settlement’ (from 8.5% to 11.2%), and 1.8% for ‘Transport’ (from 0.1% to 1.9%).

The changes in exposed land-uses suggest that coastal flood impacts could be increasingly severe in the coming decades. Furthermore, it is crucial to underscore that the affected housing areas, encompassing both informal settlements and residential settlements—the two predominant categories following ‘open areas’, are likely to suffer most from flood damage as they are located in most cases in the first line along this coastline. A closer look at the distribution of affected housing areas across coastal neighborhoods of the Port-Bouët Bay is shown in figure 11. As it can be observed, Sogefiha currently stands out as the most exposed neighborhood accounting for 86% of the housing surface exposure, trailed by Petit-Bassam (11%) and Vridi (3%). This pattern is anticipated to persist both over time and across various climate change scenarios, barring one notable exception in the year 2100 under the SSP5-8.5 scenario, where projected flooding in Vridi would lead to the inundation of substantial housing surfaces. Consequently, this would elevate Vridi to the position of the second-most exposed neighborhood, closely trailing Sogefiha in terms of housing exposure for this particular scenario.

## 5. Discussion

### 5.1. Insights

Using a GIS-based approach, the present study evaluates the current and future exposure to coastal flood hazard in the Port-Bouët Bay. This kind of assessment is critical in managing and mitigating the risks associated with coastal flooding (Sarica *et al* 2021). The study used the enhanced bathtub model (eBTM), which is a simple yet

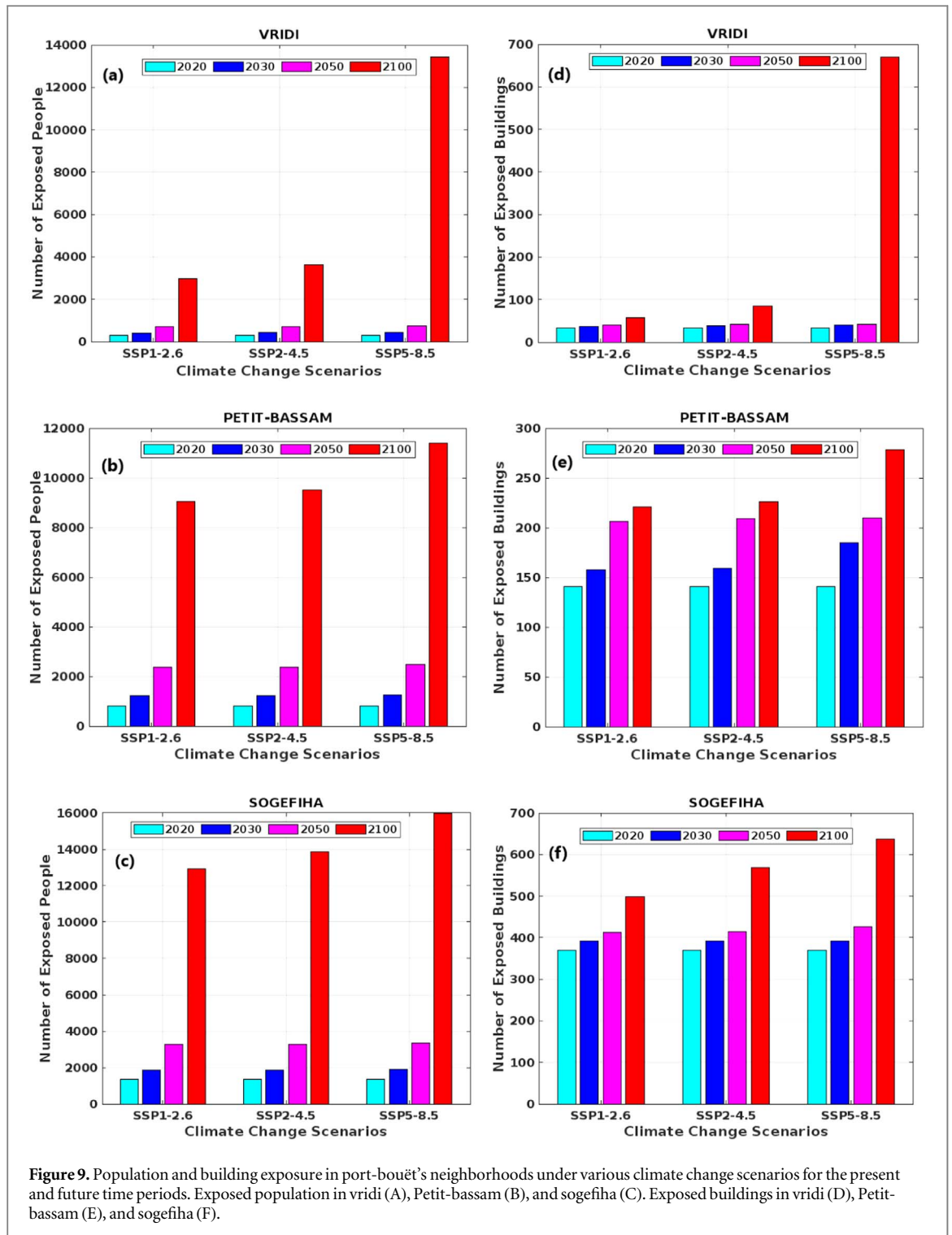
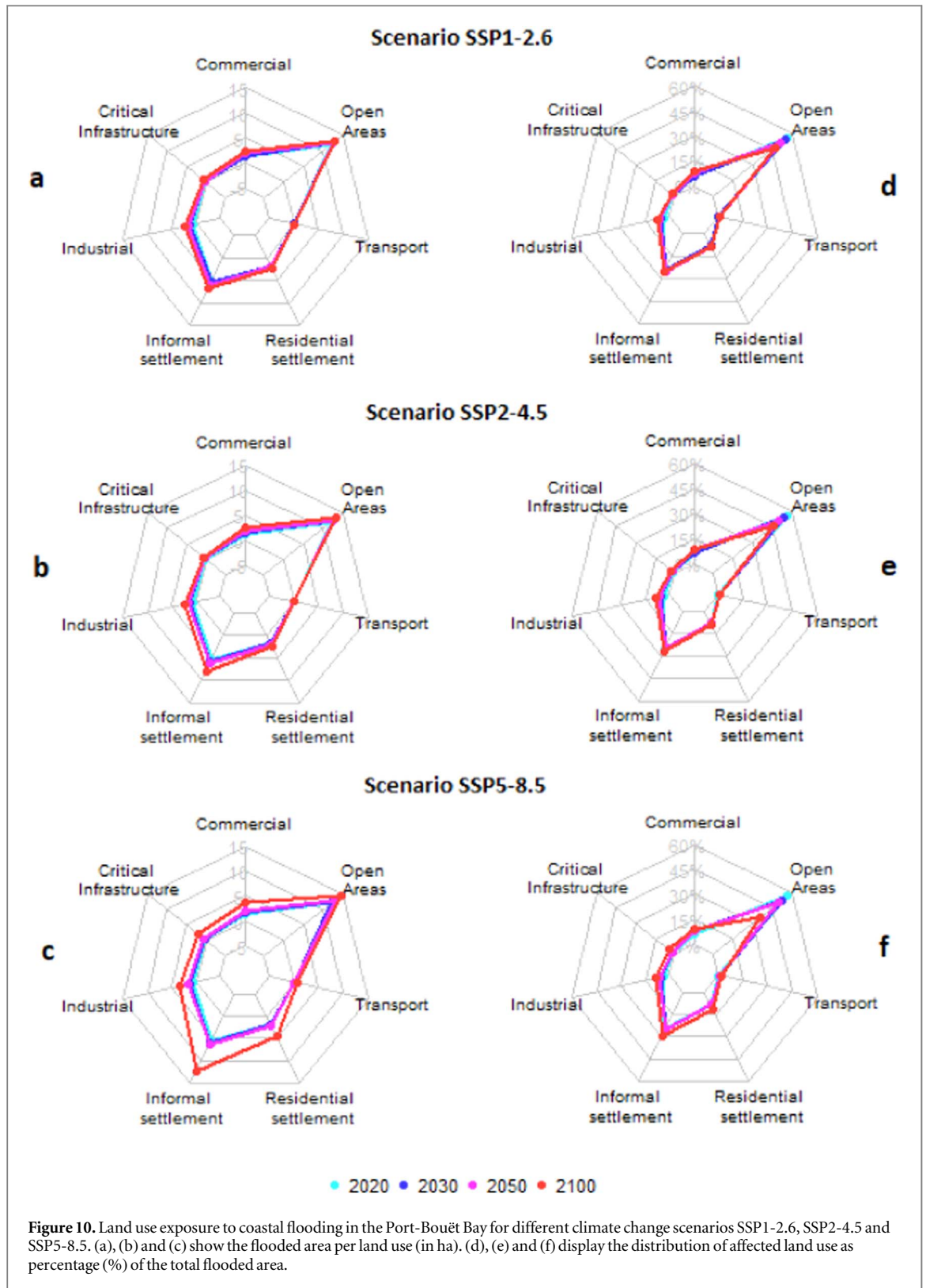


**Figure 9.** Population and building exposure in port-bouët’s neighborhoods under various climate change scenarios for the present and future time periods. Exposed population in vridi (A), Petit-bassam (B), and sogefiha (C). Exposed buildings in vridi (D), Petit-bassam (E), and sogefiha (F).

effective mapping method that yielded significant outcomes. To achieve this, we incorporated into the eBTM, a 10-meter resolution DTM and robust time-dependent extreme sea level (ESL) scenarios. This DEM, generated from the topographical data of JICA (2015), is one of the most accurate available for the area. Noteworthy that open-source DEMs with resolutions of 30–90 meters can impede mapping the extent of coastal flooding due to various errors (Wechsler 2007). As for the time-dependent ESL scenarios, they help demonstrate the significance of climate change effects on coastal flooding and their potential impacts at the different time scales considered in this study. The simulations not only provide insights on the area likely to be flooded in different climate change scenarios but also to facilitate the estimations of the number of people, buildings and surface of land-uses that could be affected in each of these scenarios

The study’s results showed that the Port-Bouët Bay is currently exposed to coastal flood phenomenon with projections showing increasing inundation surfaces and potential doubling of flood extent by 2100 under



climate change scenario SSP5-8.5. This is particularly due to topographical characteristics of the area and the unprotected coastline. Noteworthy that the flood maps obtained under current and future sea-level conditions reveal a relatively constrained flooding extent, primarily within the first 200 meters from the coastline. This flooded area, which represents only 2%–4% of the entire study area, holds particular importance due to the potential implications for coastal communities and land use. By intersecting the flood extent with population, building, and land-use data, the study provides a better understanding of the potential exposure to coastal flood hazards in Port-Bouët Bay. The examination of population and building exposure to coastal floods revealed that Port-Bouët Bay is currently exposed to a relatively significant number of people and buildings, with potential

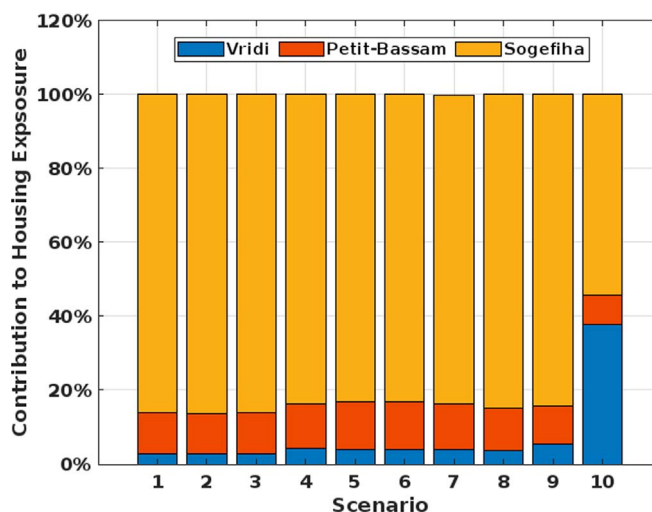


**Figure 11.** Contribution of Housing Exposure by Neighborhood in Port-Bouët Bay. The calculation considers the combined surfaces of informal settlements and residential areas. The x-axis depicts a range of climate change scenarios, spanning different timeframes and representative concentration pathways: Scenario 1 (2020), Scenario 2 (2030; SSP1-2.6), Scenario 3 (2030, SSP2-4.5), Scenario 4 (2030, SSP5-8.5), Scenario 5 (2050; SSP1-2.6), Scenario 6 (2050, SSP2-4.5), Scenario 7 (2050, SSP5-8.5), Scenario 8 (2100, SSP1-2.6), Scenario 9 (2100, SSP2-4.5), and Scenario 10 (2100, SSP5-8.5).

increases projected by 2030 and mid-century, and substantial rises by 2100. This increasing flood exposure can be attributed to the dense population and building concentration along the coastline, making the area particularly susceptible to such hazards and their potential consequences. The land-use exposure analysis indicates the predominance of exposed housing areas (both informal and residential land-use), representing 76% of the exposed land-use excluding open spaces. These findings corroborate the outcomes of larger-scale studies conducted by IMDC (2017), Muis *et al* (2017), Nicholls *et al* (2007), and the World Bank (2022). The spatial distribution of this coastal flood exposure across neighborhood indicated that the Sogefiha is the most exposed neighborhoods followed by petit-bassam and Vridi. However, a significant surge in coastal flooding in Vridi by 2100 under the SSP5-8.5 scenario could result in substantial exposure, potentially changing this above order.

## 5.2. Limitations

Given the potential for uncertainty in the study's estimations, it is vital to discuss them to acknowledge limitations and pinpoint areas for future research and improvements. In this work, uncertainties may rise from various sources: One such source is the non-variation over time in certain input datasets, such as topography, roughness, water source, and land use distribution. Though these assumptions may be valid in the short-term basis, there can introduce some uncertainties in the long-term estimations coastal flood exposure. Nevertheless, these assumptions helped to simplify the understanding of the coastal environment of Port-Bouët Bay as these types of data were not accurately available for the area.

Another source of uncertainty may arise from the model validation process. The validation of coastal flood simulations requires data on flooding characteristics collected in a safe and effective way, very shortly after flood occurrence (Molinari *et al* 2018, OPW, 2019). Unfortunately, in many coastal regions, such data is rarely available since occurrences of coastal flooding are infrequent and related information is often not documented following flood incidents, as stated by Bates (2004). In this study, model outputs were validated against observed data on coastal flood extent that were collected through surveys. However, the reliability of such validation data remains low due to the time lag between the flood occurrence and the survey. Therefore, to complement existing validation methods, it is advisable for competent authorities to explore newer data capture methods, such as citizen science (public participation in scientific research), especially during extreme events. Additionally, it is recommended to conduct regular post-coastal flood data collection and create a database to gather temporal and spatial information about historical events. Implementing these approaches can enhance model validation and minimize uncertainties in coastal flood studies along the Ivorian coasts (Bates 2004, Molinari *et al* 2018, OPW 2019, Tavares *et al* 2021).

In the course of our study, we employed the uniform disaggregation method for population distribution, evenly allocating population counts from a coarse grid to finer grid cells. Worth noting is that the obtained 30x30m resolution population maps from the 'data for goods database' already relied on high-resolution identification of inhabited areas and a comprehensive understanding of underlying population distribution

patterns. This uniform disaggregation method, serving as a simplification approach to transition from 30x30m to 10x10m resolution, effectively fulfilled the purpose of this study. However, we strongly recommend exploring alternative methods including machine learning techniques for enhancing the accuracy and granularity of population disaggregation in future coastal flood exposure assessments. Generally, flood exposure in urban areas can be associated with flood characteristics such as flood frequency, duration, depth, extent and velocity (De Moel *et al* 2009). But, the specific flood characteristics to be taken into account in exposure assessments may vary according to research objectives, methodological approach, and data quality. For Merz *et al* (2007) and Zhu *et al* (2019), flood depth is the main driver of urban flood exposure. On the other hand, DCLG (2009) suggested that flood extent alone could be adequate to identify the exposed elements to floods for spatial planning purposes. In the case of the current research, only flood extent was considered in the exposure analysis though both flood depth and extent were provided as outputs from the eBTM. This consideration is consistent with several studies recently carried out in the field of flood management (Dandapat & Panda 2018, Hadipour *et al* 2020, Jafarzadegan *et al* 2022, Stephens *et al* 2017). In this study, the omission of flood depth was based on two main factors: the unreliability of the flood depth outputs, which were not validated, and the resolution of the DEM used in the analysis, potentially affecting flood depth accuracy. Due to these limitations, we focused on other flood-related parameters confidently derived from available data. Including flood depths may require precise and current coastal land elevation data (Ward *et al* 2011), which was unavailable as the DEM used dates back to 2013. This outdated data could introduce uncertainty in the analysis. However, it is essential to recognize that incorporating water depths could have assisted in determining exposure severity. It is important to acknowledge that the present work represents an initial attempt to approximate the issue of coastal flood exposure along the Ivorian coastline. Thus, as more and accurate data becomes available, there is the potential for further improvements and considerations in this issue. To further achieve this, Ward *et al* (2011) suggests that the acquisition of LiDAR data, along with regular field campaigns, would be necessary to enhance mapping outcomes and explore other aspects of coastal flood exposure in Port-Bouët Bay. LiDAR-based high-resolution DEMs have demonstrated superior mapping capabilities for coastal flood-prone areas in comparison to other types of DEMs (Poulter and Halpin 2008, Gesch, 2009). DEMs can be divided into digital terrain models (DTMs), also known as 'bare-earth' DEMs, and digital surface models (DSMs), which capture the heights of objects on the Earth's surface such as buildings, walls and vegetation (Rogers *et al* 2020, Guth *et al* 2021). This study makes use of DTM data. However, Williams and Lück-Vogel (2020) recommend DSMs as they are based on the principle that solid structures such as buildings and walls may influence water flow patterns in urban landscapes, thereby offering protection to other structures. DSMs assist in identifying water pathways during flood events. In this context, eBTM performs better with DSMs than with DTM, as a DTM represents an unobstructed environment for water movement. Therefore, it clearly appears that LiDAR-derived high-resolution DSMs, when available and accessible for our location, could significantly enhance the present study's results. Such data could also assist in predicting future topographical changes (Zhang *et al* 2005), which are crucial for better estimating future coastal flood exposure.

## 6. Conclusions

This paper has presented an assessment of the potential trend of exposure to coastal flooding in Port-Bouët Bay under three climate change scenarios. Despite the simplicity of the methodology employed, it has provided a preliminary yet informative overview of flood-prone areas, the populations, buildings, and land use categories exposed to extreme sea level conditions, along with their distribution across the coastal neighborhoods.

In the face of some data constraints, particularly in terms of future scenarios, specific assumptions were leveraged to address these challenges while highlighting opportunities for improving data quality and model validation. Our study's results reveal a gradual increase in flood extent and exposed elements (populations, buildings and land-uses) from the present day to the close of the century. This suggests the likelihood of heightened damages and losses resulting from coastal flood hazards, particularly within informal settlements and residential areas, identified as the most exposed land use categories. Consequently, coastal flood hazards would emerge as the most substantial climate change impact in the study area in the forthcoming decades.

The findings of this study are very useful to be applied in adaptation strategies. They can provide researchers and decision-makers with insights into the potential impacts of coastal flooding both in the present and in the future conditions. This information not only holds potential for revising and planning future adaptation programs but also serves as a foundational baseline for upcoming studies, potentially inspiring the pursuit of enhanced data collection and analysis. By identifying exposed areas and assets exposed to coastal flooding, we can raise awareness and readiness levels across various decision-making tiers, including residents, emergency responders, and stakeholders. This proactive approach might involve promoting the implementation of flood protection measures and the development of comprehensive emergency response plans for flood-related

disasters. Furthermore, the spatial disaggregation of findings down to the neighborhood scale offers the advantage of tailored risk management and targeted interventions, thus enhancing local resilience.

## Acknowledgments

The authors would like to acknowledge the West African Climate Change and Adapted Land Use (WASCAL), funded by the German Federal Ministry for Education and Research, for providing financial support to the corresponding author, to conduct this research as part of his postgraduate studies.

## Data availability statement

All data that support the findings of this study are included within the article (and any supplementary files).

## Funding

This research received no external funding.

## Conflict of interest

The authors declare no competing interest.

## ORCID iDs

Marcel Kouakou  <https://orcid.org/0000-0001-8318-4084>

## References

- Al Ruheili A and Boluwade A 2023 Towards quantifying the coastal vulnerability due to natural hazards using the inVEST coastal vulnerability model *Water* **15** 380
- Alizad K, Hagen S C, Medeiros S C, Bilskie M V, Morris J T, Balthis L and Buckel C A 2018 Dynamic responses and implications to coastal wetlands and the surrounding regions under sea level rise *PLoS One* **13** e0205176
- Amante C 2018 *Consideration of elevation uncertainty in coastal flood models* University of Colorado, Boulder (<https://doi.org/10.13140/RG.2.2.11549.15848>)
- Bates P D 2004 Remote sensing and flood inundation modelling *Hydrol. Processes* **18** 2593–7
- Castillo M E, Baldwin E M, Casarin R S, Vanegas G P and Juaréz M A 2012 Characterization of risks in coastal zones: a review *Clean - Soil, Air, Water* **40** 894–905
- Center for International Earth Science Information Network - CIESIN 2018 Documentation for the Gridded Population of the World, Version 4 (GPWv4), Revision 11 Data Sets *NASA Socioeconomic Data and Applications Center (SEDAC)* Palisades NY:
- Dandapat K and Panda G K 2018 A geographic information system-based approach of flood hazards modelling, Paschim Medinipur district, West Bengal, India *Jamba: Journal of Disaster Risk Studies* **10** 1–7
- D'Arcy E, Tawn J A and Sifnioti D E 2022 Accounting for climate change in extreme sea level estimation *Water (Switzerland)* **14** 1–21
- DCLG 2009 *Planning policy statement 25: development and flood risk practice guide* Department for Communities and Local Government, London, UK 1–182
- De Moel H, Van Alphen J and Aerts J C J H 2009 Flood maps in Europe—methods, availability and use *Nat. Hazards Earth Syst. Sci.* **9** 289–301
- Dube K, Nhamo G and Chikodzi D 2022 Flooding trends and their impacts on coastal communities of Western Cape Province, South Africa *GeoJournal* **87** 453–68
- Fang J and Shi P 2021 Research progress and prospect of coastal flood disaster risk assessment against global climate change *Journal of Geography and Cartography* **4** 102–16
- Facebook Connectivity Lab - FCL and Center for International Earth Science Information Network - CIESIN - Columbia University 2022 High resolution settlement layer (HRSL) *Source imagery for HRSL, Maxar*. Accessed 31 March 2022
- Fereshtehpour M and Karamouz M 2018 DEM resolution effects on coastal flood vulnerability assessment: deterministic and probabilistic approach *Water Resour. Res.* **54** 4965–82
- Fox-Kemper B et al 2021 Cryosphere and sea level change *Climate Change 2021: The Physical Science Basis. Contribution of Working Group I to the Sixth Assessment Report of the Intergovernmental Panel on Climate Change* ed V Masson-Delmotte et al (Cambridge University Press)
- Gallien T W, Sanders B F and Flick R E 2014 Urban coastal flood prediction: Integrating wave overtopping, flood defenses and drainage *Coastal Eng.* **91** 18–28
- Garner G G, Palmer M D, Smith C, Fox-Kemper B et al 2021a IPCC AR6 Sea-Level Rise Projections Version 20210809 Available online: <https://sealevel.nasa.gov/ipcc-ar6-sea-level-projection-tool> (accessed on 31 January 2022)
- Garner G G, Kopp R E, Hermans T, Slangen A B A, Koubbe G, Turilli M, Jha S, Edwards T L, Levermann A, Nowicki S et al 2021b Framework for Assessing Changes To Sea-level (FACTS) *Geoscientific Model Development*.
- Gesch D B 2009 Analysis of lidar elevation data for improved identification and delineation of lands vulnerable to sea-level rise *Journal of Coastal Research* **53** 49–58

- Gesch D B 2018 Best practices for elevation-based assessments of sea-level rise and coastal flooding exposure *Front. Earth Sci.* **6** 230
- Guth P L et al 2021 Digital elevation models: terminology and definitions *Remote Sensing* **13** 1–19
- Hadipour V, Vafaie F and Deilami K 2020 Coastal flooding risk assessment using a GIS-based spatial multi-criteria decision analysis approach *Water* **12** 2379
- Hague B S, Jones D A, Jakob D, McGregor S and Reef R 2022 Australian coastal flooding trends and forcing factors *Earth's Future* **10** 1–20
- Hallegatte S, Green C, Nicholls R J and Corfee-Morlot J 2013 Future flood losses in major coastal cities *Nat. Clim. Change* **3** 802–6
- HARPIS-SL 2022 *Flood Exposure, Vulnerability and Risk*. (INTEGREMS) <https://harpis-sl.website/index.php/hazard-assessment/natural/flood/fldexposure-vulnerability-and-risk-assessment>
- Idier D, Rohmer J, Pedreros R, Le Roy S, Lambert J, Louisor J, Le Cozannet G and Le Cornec E 2020 Coastal flood: a composite method for past events characterisation providing insights in past, present and future hazards—joining historical, statistical and modelling approaches *Nat. Hazards* **101** 465–501
- IMDC 2017 *Coût de la dégradation environnementale, évaluation du risque multi-aléas et analyse coût-bénéfice des solutions pour la zone côtière. D7d: Analyse coût-bénéfice des options de RRC et ACC sélectionnées pour la Côte d'Ivoire—secteur C15 Port Bouët I/RA/12148/17.118/ABO* International Marine & Dredging Consultants
- INS 2014 *Résultats Globaux du Recensement général de la population et de l'habitat (R.G.P.H.) 2014* Institut National de la Statistique 1–12
- INS 2021 *Résultats Globaux Recensement général de la population et de l'habitat (R.G.P.H.) 2021* Institut National de la Statistique 1–37
- IPCC 2021 *Climate Change 2021 The Physical Science Basis Climate Change 2021 Contribution of Working Group I to the Sixth Assessment Report of the Intergovernmental Panel on Climate Change* ed V Masson-Delmotte et al (Cambridge University Press) (<https://doi.org/10.1017/9781009157896>)
- Jafarzadegan K, Muñoz D F, Moftakhari H, Gutenson J L, Savant G and Moradkhani H 2022 Real-time coastal flood hazard assessment using DEM-based hydrogeomorphic classifiers *Nat. Hazards Earth Syst. Sci.* **22** 1419–35
- Jeer S and Bain B 1997 *Traditional Color Coding for Land Uses* American Planning Association 1–7
- JICA 2015 *Digital topographic mapping project for urban infrastructure development (A Fast Track Project)* Japan International Cooperation Agency 1–177
- Kirwan M L and Megonigal J P 2013 Tidal wetland stability in the face of human impacts and sea-level rise *Nature* **504** 53–60
- Kouakou M, Bonou F, Gnanadi K, Djagoua E, Idrissou M and Abunkudugu A 2023 Determination of current and future extreme sea levels at the local scale in port-Bouët Bay (Côte d'Ivoire) *Journal of Marine Science and Engineering* **11** 756 MDPI AG. Retrieved from
- Kulp S A and Strauss B H 2019 New elevation data triple estimates of global vulnerability to sea-level rise and coastal flooding *Nat. Commun.* **10** 4844
- Lakshmi A 2012 Coastal ecosystem services & human wellbeing *Indian J. Med. Res.* **153** 382–7
- Merz B, Thielen A H and Gocht M 2007 Flood risk mapping at the local scale: concepts and challenges *Flood Risk Management in Europe* ed S Begum et al (Springer) vol 23, pp 231–51
- Molinari D, De Bruijn K M, Jesica T, Aronica G T, Bouwer M, Molinari D, De Bruijn K M, Castillo- J T, Aronica G T and Bouwer L M 2018 Validation of flood risk models: current practice and possible improvements *Int. J. Disaster Risk Reduct.* **33** 1–21
- Muis S, Verlaan M, Nicholls R J, Brown S, Hinkel J, Lincke D, Vafeidis A T, Scussolini P, Winsemius H C and Ward P J 2017 Earth's Future A comparison of two global datasets of extreme sea levels and resulting flood exposure Earth's Future *Earth's Future* **5** 379–92
- Neumann B, Vafeidis A T, Zimmermann J and Nicholls R J 2015 Future coastal population growth and exposure to sea-level rise and coastal flooding - A global assessment *PLoS One* **10** e0118571
- Neumann T and Ahrendt K 2013 *Comparing the 'bathtub method' with mike 21 HD flow model for modelling storm surge inundation: case study kiel fjord* 22 RADOST 1–45
- Nicholls R J, Hanson S, Herweijer C, Patmore N, Hallegatte S, Corfee-Morlot J, Chateau J and Muir-Wood R 2007 *Ranking of the World's cities most exposed to coastal flooding today and in the future ENV/WKP(2007)1* Organisation for Economic Co-operation and Development - OECD 1–11 Permanent Link: <http://dpanther.fiu.edu/dpService/dpPurlService/purl/FI15061848/00001>
- OPW 2019 *Food Data Collector's Handbook: A Practical Guide to Flood Data Collection*. (The Stationery Office) <https://gov.ie/en/collection/a06c18-flood-event-data-collection/>
- Percival S and Teeuw R 2019 A methodology for urban micro-scale coastal flood vulnerability and risk assessment and mapping *Nat. Hazards* **97** 355–377
- Poulter B and Halpin P N 2008 Raster modelling of coastal from sea-level rise *Int. J. Geogr. Inf. Sci.* **22** 167–82
- Rogers S R, Manning I and Livingstone W 2020 Comparing the spatial accuracy of digital surface models from four unoccupied aerial systems: photogrammetry versus lidar *Remote Sensing* **12** 1–17
- Sadia C 2014 Risque climatique et réactivité des populations urbaines vulnérabilisées face à la montée des eaux de mer à Gonzagueville, Abidjan (Côte d'Ivoire) *VertigO - la revue électronique en sciences de l'environnement* **14**
- Sarica G M, Zhu T, Jian W, Lo E Y-M and Pan T-C 2021 Spatio-temporal dynamics of flood exposure in Shenzhen from present to future *Urban Analytics and City Science* **48** 1011–24
- Seenath A, Wilson M and Miller K 2016 Hydrodynamic versus GIS modelling for coastal flood vulnerability assessment: which is better for guiding coastal management? *Ocean Coast. Manage.* **120** 99–109
- Sirko W, Kashubin S, Ritter M, Annkah A, Bouchareb Y S E, Dauphin Y, Keyzers D, Neumann M, Cisse M and Quinn J 2021 *Continental-Scale Building Detection from High Resolution Satellite Imagery*. 1–15 <http://arxiv.org/abs/2107.12283>
- Steffen W L, William L, Hunter J, Hughes L and Climate Council 2014 *Counting the Costs: Climate Change and Coastal Flooding*. The Climate Council of Australia Limited (<https://climatecouncil.org.au>) 1–73
- Stephens S A, Bell R G and Lawrence J 2017 Applying principles of uncertainty within coastal hazard assessments to better support coastal adaptation *Journal of Marine Science and Engineering* **5** 40
- Tavares A O, Barros J L, Freire P, Santos P P, Perdiz L and Fortunato A B 2021 A coastal flooding database from 1980 to 2018 for the continental Portuguese coastal zone *Appl. Geogr.* **135** 1–17
- United Nations 2017 Factsheet: people and oceans general *The Ocean Conference (New York, 5-9 June 2017)* 1–2
- Vitousek S, Barnard P L, Fletcher C H, Frazer N, Erikson L and Storlazzi C D 2017 Doubling of coastal flooding frequency within decades due to sea-level rise *Sci. Rep.* **7** 1399
- Vousdoukas M I, Mentaschi L, Voukouvalas E, Bianchi A, Dottori F and Feyen L 2018 Climatic and socioeconomic controls of future coastal flood risk in Europe *Nat. Clim. Change* **8** 776–80
- Wahl T, Haigh I D, Nicholls R J, Arns A, Dangendorf S, Hinkel J and Slangen A B A 2017 Understanding extreme sea levels for broad-scale coastal impact and adaptation analysis *Nat. Commun.* **8** 1–12
- Ward P J, Marfai M A, Yulianto F, Hizbaron D R and Aerts J C J H 2011 Coastal inundation and damage exposure estimation: a case study for Jakarta *Nat. Hazards* **56** 899–916

- Wechsler SP 2007 Uncertainties associated with digital elevation models for hydrologic applications: A review *Hydrol. Earth Syst. Sci.* **11** 1481–500
- Williams L L 2019 *Coastal Inundation (Enhanced Bathtub Model (eBTM))*. (Department of Environment., Forestry and fisheries)
- Williams L L 2020 *Coastal Inundation (eBTM with Variable Roughness Input)*. (Department of Environment., Forestry and fisheries)
- Williams L L and Lück-Vogel M 2020 Comparative assessment of the GIS based bathtub model and an enhanced bathtub model for coastal inundation *Journal of Coastal Conservation* **24** 1–15
- World Bank 2020 *Effects of climate change on coastal erosion and flooding in Benin, Côte d'Ivoire, Mauritania, Senegal, and Togo* Technical Report May 2020 The World Bank, Washington, DC 1-127
- World Bank 2022 *Compendium: Coastal Management Practices in West Africa - Existing and Potential Solutions to Control Coastal Erosion (Prevent Flooding and Mitigate Damage to Society)* <https://openknowledge.worldbank.org/handle/10986/37351>
- World Meteorological Organization 2013 *Integrated Flood Management Tools Series: Coastal and Delta Flood Management* 11 11 WMO ([www.wmo.int](http://www.wmo.int))
- Wu W, Zhou Y and Tian B 2017 Coastal wetlands facing climate change and anthropogenic activities: A remote sensing analysis and modelling application *Ocean Coast. Manag.* **138** 1–10
- Zhang K, Whitman D, Leatherman S and Robertson W 2005 Quantification of beach changes caused by hurricane Floyd along Florida's atlantic coast using airborne laser surveys *J. Coast. Res.* **21** 123–34
- Zhu X, Dai Q, Han D, Zhuo L, Zhu S and Zhang S 2019 Modeling the high-resolution dynamic exposure to flooding in a city region *Hydrol. Earth Syst. Sci.* **23** 3353–72